Sensors and Actuators A 255 (2017) 46–53

Contents lists available at ScienceDirect

Sensors and Actuators A: Physical

journal homepage: www.elsevier.com/locate/sna

Bioinspired tactile sensor for surface roughness discrimination

Zhengkun Yi[a,b], Yilei Zhang[a,*], Jan Peters[b,c]

[a] School of Mechanical & Aerospace Engineering, Nanyang Technological University, Singapore
[b] Intelligent Autonomous Systems Lab, Department of Computer Science, Technische Universitaet Darmstadt, Germany
[c] Max Planck Institute for Intelligent Systems, Tuebingen, Germany

ARTICLE INFO

Article history:
Received 4 August 2016
Received in revised form 31 October 2016
Accepted 20 December 2016
Available online 5 January 2017

Keywords:
Surface roughness discrimination
Bioinspired fingertip
Feature extraction
Machine learning
Tactile sensor

ABSTRACT

Surface texture discrimination using artificial tactile sensors has attracted increasing attentions in the past decade as it can endow robot systems with a key missing ability. However, as a major component of texture, roughness has rarely been explored. This paper presents an approach for tactile surface roughness discrimination, which includes two parts: (1) design and fabrication of a bioinspired artificial fingertip, and (2) tactile signal processing for tactile surface roughness discrimination. The bioinspired fingertip is comprised of two polydimethylsiloxane (PDMS) layers, a polymethyl methacrylate (PMMA) bar, and two perpendicular polyvinylidene difluoride (PVDF) film sensors. This artificial fingertip mimics human fingertips in three aspects: (1) Elastic properties of epidermis and dermis in human skin are replicated by the two PDMS layers with different stiffness, (2) The PMMA bar serves the role analogous to that of a bone, and (3) PVDF film sensors emulate Meissner's corpuscles in terms of both location and response to the vibratory stimuli. Various extracted features and classification algorithms including support vector machines (SVM) and *k*-nearest neighbors (*k*NN) are examined for tactile surface roughness discrimination. Eight standard rough surfaces with roughness values (Ra) of 50 μm, 25 μm, 12.5 μm, 6.3 μm, 3.2 μm, 1.6 μm, 0.8 μm, and 0.4 μm are explored. By simply sliding the sensor on the surfaces without any load and speed controller, we found that the highest classification accuracy of (82.6 ± 10.8) % can be achieved using solely one PVDF film sensor with *k*NN (*k* = 9) classifier and the standard deviation feature, i.e., the developed approach is very affordable, robust and suitable for real time surface roughness evaluation.

1. Introduction

Surface texture is an important object property and can significantly affect the friction characteristics, wear resistance, and fatigue life of components [1]. Tremendous efforts have been made to recognize the surface texture using artificial tactile sensors or artificial fingers [2–5]. For example, a commercial electret microphone embedded in a silicone rubber was used to classify 18 surface textures [2]. By aid of a supervised learning vector quantization (LVQ) classifier, a classification accuracy of 93% was achieved. Muhammad et al. [3], developed a capacitive tactile sensor array to recognize fabrics including poly cotton and nylon. Oddo et al. [6], fabricated a 2 × 2 tactile piezoresistive sensor array based on microfabrication technology, which was embedded in a polymeric packaging with fingerprint-like structures. The density of the tactile sensing elements was considered to be comparable to that of human SA-I mechanoreceptors. Three gratings with 400 μm, 440 μm, and 480 μm spatial periods were explored. The wavelet and cross-wavelet transforms were performed to extract tactile features, and a classification accuracy of 97.6% was achieved by a *k*-Nearest Neighbors (*k*NN) classifier. Peiner et al. [7], developed a tactile cantilever sensor intended for high-aspect-ratio micrometrology with a resolution of 10–20 nm when scanning at a velocity of 0.63 mm/s. However, this sensor was prone to wear or damage.

Surface texture is defined by multiple characteristics such as roughness and hardness. Although tactile surface texture has been intensively investigated, surface roughness as a major component of surface texture is rarely explored. Current approaches to measure surface roughness could be divided into two categories [8]: contacting methods and non-contacting methods. The contacting methods are relatively immune to external interference as they depend mainly on the repulsive mechanical contact with the test surfaces. However, the stylus tip is prone to wear, and may cause scratches on the test surface as well. Compared to contacting methods, non-contacting methods measure the surface in a non-destructive way, but suffer from the limitations such as high sensitivity to surface slope and height.

* Corresponding author.
E-mail addresses: YLZHANG@ntu.edu.sg, zhangyilei@gmail.com (Y. Zhang).

http://dx.doi.org/10.1016/j.sna.2016.12.021
0924-4247/

Human beings possess the ability to sensitively perceive different materials [9], but the question remains as to how human beings encode the surface roughness during the physical finger-surface interactions. Extensive researches have been conducted to investigate the mechanisms underlying the perception of surface roughness [10–12]. Connor et al. [10], proposed that the neural coding of tactile texture is closely related to the spatial variations in slowly adapting (SA) mechanoreceptive afferents, which was limited to the coarse surfaces with element spaces of >1 mm. Yoshioka et al. [11] extended Connor et al.'s work by studying the neural coding mechanisms for the roughness perception of finely textured surface, and found that there was a consistent relationship between human judgements of fine surface roughness and slowly adapting type I (SA-I) spatial variations. Libouton et al. [12], indicated that the tactile roughness discrimination relies mainly on vibration sensitive afferents. The fast adapting type I (FA-I) mechanoreceptors (Meissner's corpuscles) and the fast adapting type II (FA-II) mechanoreceptors (Pacinian corpuscles) are generally regarded to be responsible for modulating the vibratory stimuli occurring at the interface of explored surfaces and the fingers [13]. Although many neurophysiological studies of the roles of mechanoreceptors have appeared, it is still an open question as to which mechanoreceptor plays a significant role. In this paper, we provide an approach to investigate surface roughness recognition with a biomimetic fingertip, which mimics the mechanical properties of FA-I mechanoreceptors. We expect this platform could provide new insights into the neurophysiological study.

The main contribution in this paper is a tactile surface roughness recognition method using a biologically inspired artificial fingertip. The artificial fingertip is designed and fabricated with two distinct polydimethylsiloxane (PDMS) layers. The inner layer is much softer than the outer layer. A polymethyl methacrylate (PMMA) bar is located in the center of this fingertip and plays the role similar to that of the bone in human fingertips. Inspired by Meissner's corpuscles in terms of both the distribution in human fingertip and the response to the vibration, two perpendicular polyvinylidene difluoride (PVDF) film sensors were placed beneath the outer PDMS layer to provide the sensory information. Both the statistical and spectral features are examined with the purpose of figuring out a good feature candidate for surface roughness discrimination. Unlike prior designs such as [6], which mimicked only SA-I mechanorecepotors (Merkel mechanorecepotors), our work reproduces the surface roughness perception ability of Meissner's corpuscles (FA-I mechanoreceptors). Another related approach [3] achieved roughness discrimination by assessing the peak frequency of frequency spectrum generated by capacitive sensors, but no other features were evaluated. The design of the artificial fingertip for our method differs from the previous work [14], where the receptors are randomly distributed. The regular arrangement of tactile sensing elements in our design is much easier to repeat and more likely to be adopted in commercial production.

The proposed approach is illustrated in Fig. 1 and the remainder of this paper is organized as follows. The design and fabrication of a biological inspired fingertip are described in Section 2. Subsequently, we give a detailed description of tactile signal processing of surface roughness discrimination in Section 3, which is followed by Section 4 of experimental setup and protocol. We then present the results and discussion in Section 5. Finally, the conclusion is described in Section 6.

2. Design and fabrication of an artificial fingertip

This section describes the approach to develop a bioinspired fingertip. We briefly present the working mechanism of piezoelectric sensors. Subsequently, we give a detailed design of the artificial fingertip to mimic FA-I mechanoreceptors. We then show the protocol of how to fabricate it.

2.1. Piezoelectric PVDF film sensors

Piezoelectric materials generate electrical charges when the crystal lattice is deformed under mechanical force and the generated charges are directly proportional to the mechanical stress [15]. However, the generated electric charges decay with a time constant that is determined by the internal impedance and dielectric constant of the piezoelectric material. A collection of tactile sensors have been developed by taking advantage of the piezoelectric effect [16–19]. These piezoelectric sensors exhibit a very good high-frequency response, which makes them extremely suitable for measuring vibrations. PVDF film is a classic example of piezoelectric polymer that is widely used as tactile sensors [20–22], where the lowest frequency measurable with piezoelectric PVDF film is in the order of about 0.01 Hz. In our previous work, the capability of a PVDF film sensor to mimic tactile FA-I afferent has been successfully

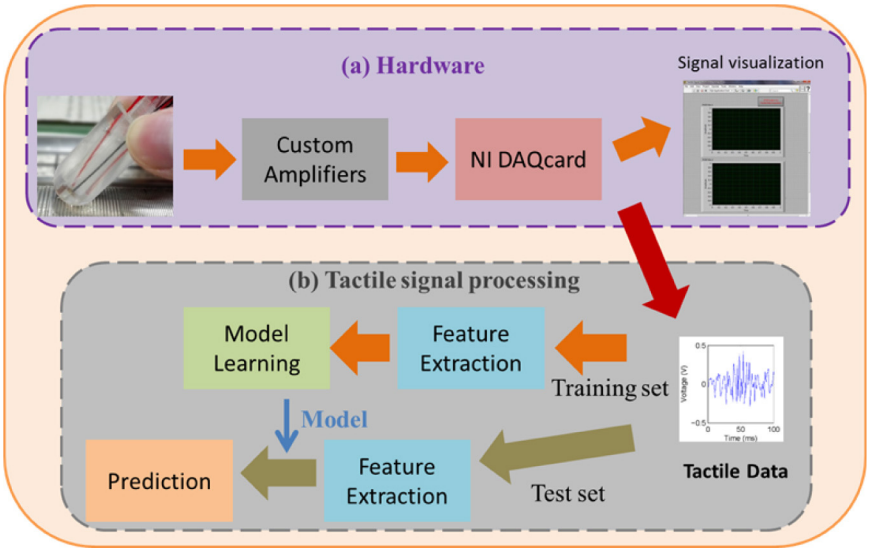

Fig. 1. Surface roughness discrimination approach with a bioinspired artificial fingertip. The approach consists of (a) hardware to acquire the tactile data and (b) tactile signal processing for surface roughness discrimination.

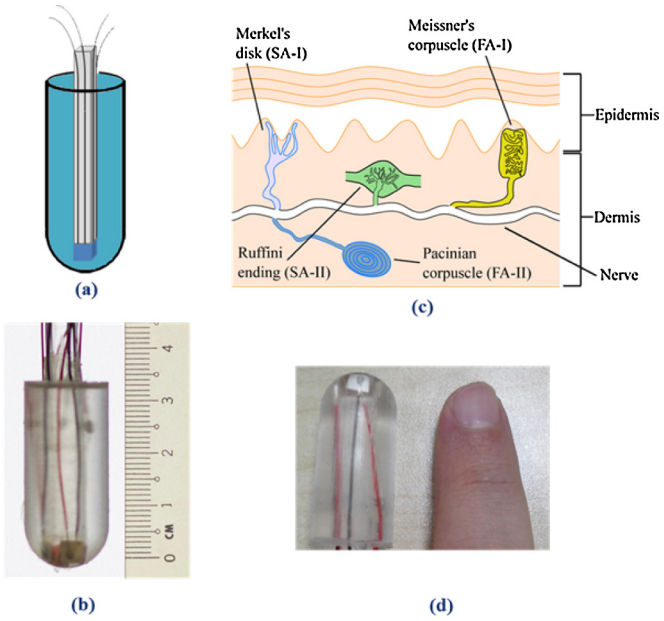

Fig. 2. Structures of (a) the designed artificial fingertip, (b) a developed artificial fingertip, (c) structure of human fingertip, and (d) artificial vs. human fingertip. The structures of both human and artificial fingertips contain two layers with different hardness, and a bone.

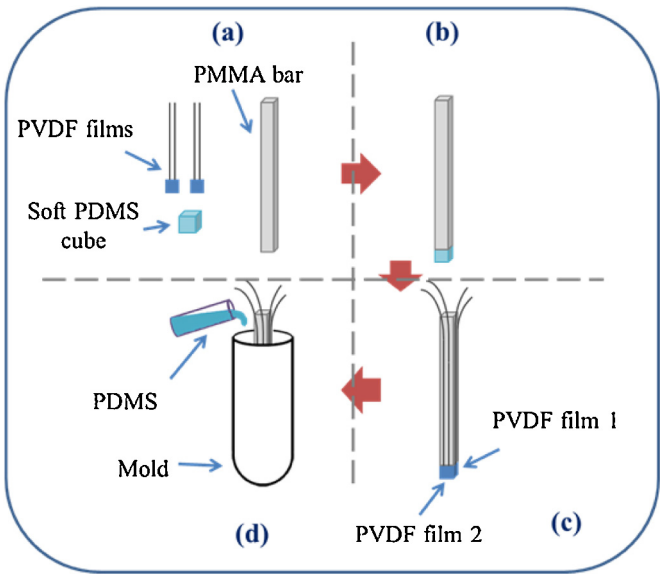

Fig. 3. The protocol of fabricating an artificial fingertip. (a) Components for fabricating an artificial fingertip. (b) A soft cured PDMS was bonded to the tip of a PMMA bar. (c) Two PVDF film sensors were arranged perpendicularly on the top of the PDMS cube. (d) The bar was inserted a mold of size resembles human fingertips; then PDMS mixed at a 10:1 mixing ratio was cast into it.

demonstrated by employing spiking neuron models and the model outputs agree reasonably well with biological measurements under the vibratory stimuli [23].

2.2. Structure of an artificial fingertip

Fig. 2 illustrates the structures of the designed artificial fingertip and human fingertip. The structure of our designed artificial fingertip resembles that of a human fingertip, which is comprised of epidermis, dermis, and a bone. The skin of human beings [24] is inherently elastic and consists of two layers, i.e., the epidermis and dermis. The hardness of the epidermis is higher than that of the dermis. In this paper, we mimic skin's elastic properties using polydimethylsiloxane (PDMS) elastomer. The hardness difference between epidermis and dermis is emulated by altering the base to curing agent mixing ratio. A polymethyl methacrylate (PMMA) bar serves the role comparable to that of a bone. In addition, the similar locations of Meissner's corpuscles, which lie just beneath the epidermis [13], are replicated by embedding the PVDF films between the two PDMS layers.

2.3. Protocol of fabricating an artificial fingertip

The protocol of fabricating the designed artificial fingertip is shown in Fig. 3. A commercial 28 μm-thick PVDF film (1-1003703-4, Measurement Specialties, USA) was cut into a desired size as small as 4 mm × 4 mm, and electrodes are bonded using a conductive paste. The soft PDMS cube is prepared by mixing 20 parts of silicone elastomer base to 1 part of curing agent (SYLGARD, Dow Corning, USA). A cuboid PMMA bar with a size of 4 mm × 4 mm × 45 mm is obtained by cutting a PMMA sheet using a laser cutting machine. The soft cured PDMS cube is bonded to either end of the PMMA bar (Fig. 3(b)). Two PVDF film sensors are then arranged perpendicularly on the top of the PDMS cube (Fig. 3(c)). The PMMA bar incorporated with a soft cured PDMS cube and PVDF films sensor was inserted in to a mold with a size comparable to human fingertips; then PDMS mixed at a 10:1 mixing ratio was cast into the mold (Fig. 3(d)). Subsequently, the mold was put into a vacuum chamber in order to degas, and baked in an oven to complete the polymerization. The Young's modulus of the outer and inner PDMS with curing time of 1 h are about 0.435 MPa and 0.147 MPa respectively [25].

Table 1
Extracted features from tactile signals.

Index	Feature type
1	Standard deviation (SD)
2	Statistical features (SF)
3	Signal roughness parameter Ra (SRa)
4	Power spectral magnitudes (PSM)
5	Combined feature 1 (SD + PSM)
6	Combined feature 2 (SF + PSM)
7	Combined feature 3 (SRa + PSM)

3. Tactile signal processing of surface roughness discrimination

In this section, statistical machine learning approaches are employed to interpret the tactile signals. First, feature extraction from tactile signals is performed. We then apply two distinct classifiers to discriminate surface roughness.

3.1. Feature extraction

Feature extraction is critical for successful pattern recognition. Hand-crafted features such as Mel-frequency cepstral coefficients (MFCCs) [26] in speech recognition and Scale-invariant feature transform (SIFT) [27] in image processing are demonstrated to be powerful in practice. In contrast, feature extraction from tactile signals is far from mature due to many reasons such as the diversity of the working principles of tactile sensors. In this paper, several approaches for tactile feature extraction from PVDF film sensors are compared in order to figure out a good feature candidate for tactile surface roughness discrimination. Table 1 describes the distinct features used in this paper.

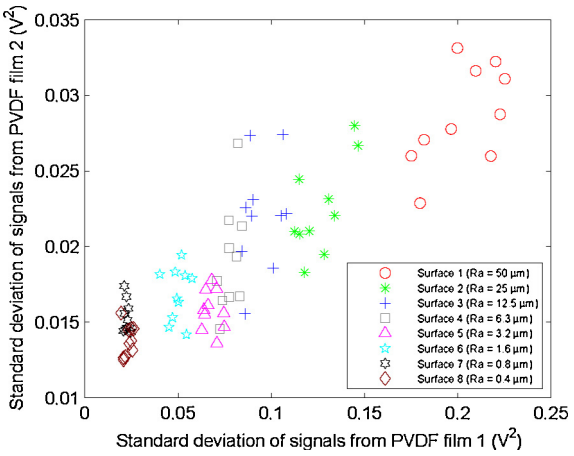

Fig. 4. Standard deviation features extracted from tactile signals of two PVDF films when laterally sliding on eight test surfaces with various roughness values.

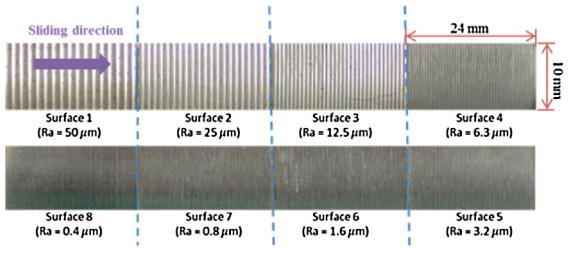

Fig. 5. Eight solid nickel test surfaces with roughness values *Ra* of 50 μm, 25 μm, 12.5 μm, 6.3 μm, 3.2 μm, 1.6 μm, 0.8 μm, and 0.4 μm were explored. The lateral sliding direction of the artificial fingertip along the test surface during the conducted experiments is indicated by an arrow.

3.1.1. Standard deviation (SD)

The standard deviation is shown to be a promising feature for material texture classification [14]. Given the close relationship between material texture and roughness, the standard deviation is used as a feature for surface roughness recognition. Standard deviation features extracted from tactile signals of two PVDF films when laterally sliding on eight surfaces (see Section 4) with various roughness values are illustrated in Fig. 4.

3.1.2. Statistical features (SF)

The SD feature can be extended to statistical features by introducing high-order moments. Specifically, the statistical features are defined as statistical moments of the tactile time series signals, which contain standard deviation, skewness, and kurtosis. Some similar features have already been used for vibration sensing [28] and local tactile shape discrimination [29].

3.1.3. Signal roughness parameter Ra (SRa)

Inspired by the surface roughness parameters, signal roughness parameters can be defined in a similar way. In this work, we use signal roughness parameter Ra as a feature type, which can be regarded as a type of statistical features as well.

3.1.4. Power spectral magnitudes (PSM)

A set of power spectral magnitudes is employed as the tactile features. It is calculated by averaging the power spectral density over the desired sub-band. Spectral power magnitudes are reported to achieve good performance on both electromyography (EMG) [30] and electroencephalogram (EEG) applications [31]. In this paper, the calculation of PSM is implemented on the whole band.

3.1.5. Combined features

Single feature may not has the same discriminative power for all classes [32]. Therefore, it could be better to combine a set of diverse features. In this paper, the feature combination is achieved by concatenating several features, which results in three additional combined features: SF + PSM, SD + PSM, and SRa + PSM. It is worth noting that a better performance could be obtained through non-linear feature combination [33].

3.2. Classification algorithms

Two classification algorithms are evaluated in this paper: Support Vector Machines (SVM) and *k*-Nearest Neighbors (*k*NN). These two methods have met with significant success in numerous real world classification tasks [34–36].

3.2.1. Support vector machines (SVM)

Support vector machines are developed from statistical learning theory [37], and have been applied in many applications in tactile sensing, such as slip detection [36], object shape recognition [29] and object texture discrimination [34]. Support vector machines are discriminative models which are aimed at finding a hyperplane to maximize the margin among classes. Kernel tricks facilitate the data processing in high dimensional spaces. Both linear SVM with the kernel function $K(\mathrm{x}_i, \mathrm{x}_j) = \mathrm{x}_i^T \mathrm{x}_j$ and radial basis function (RBF) SVM with the kernel function $K\left(\mathbf{x_i}, \mathbf{x_j}\right) = \exp\left(-\gamma \|\mathbf{x_i} - \mathbf{x_j}\|^2\right)$, where γ is the kernel parameter, are evaluated. The cost parameter C and kernel parameter γ for SVM-RBF are optimized by executing a grid search during the cross-validation procedure. The multi-class SVM classification used in this paper is based on "one-against-all" scheme [38]. The classifier implemented in this work comes from the LIBSVM library [39].

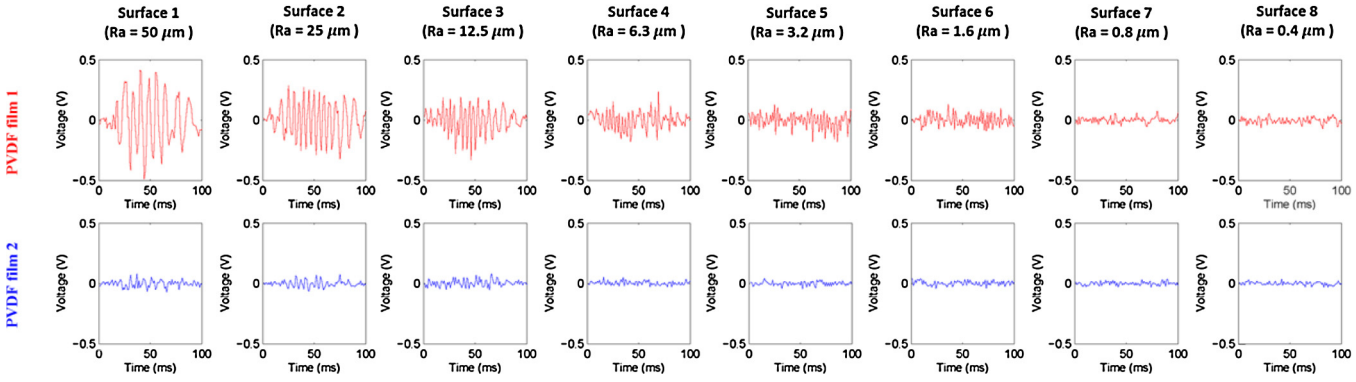

Fig. 6. Typical tactile signals generated by two PVDF films when laterally sliding on eight test surfaces with various roughness values.

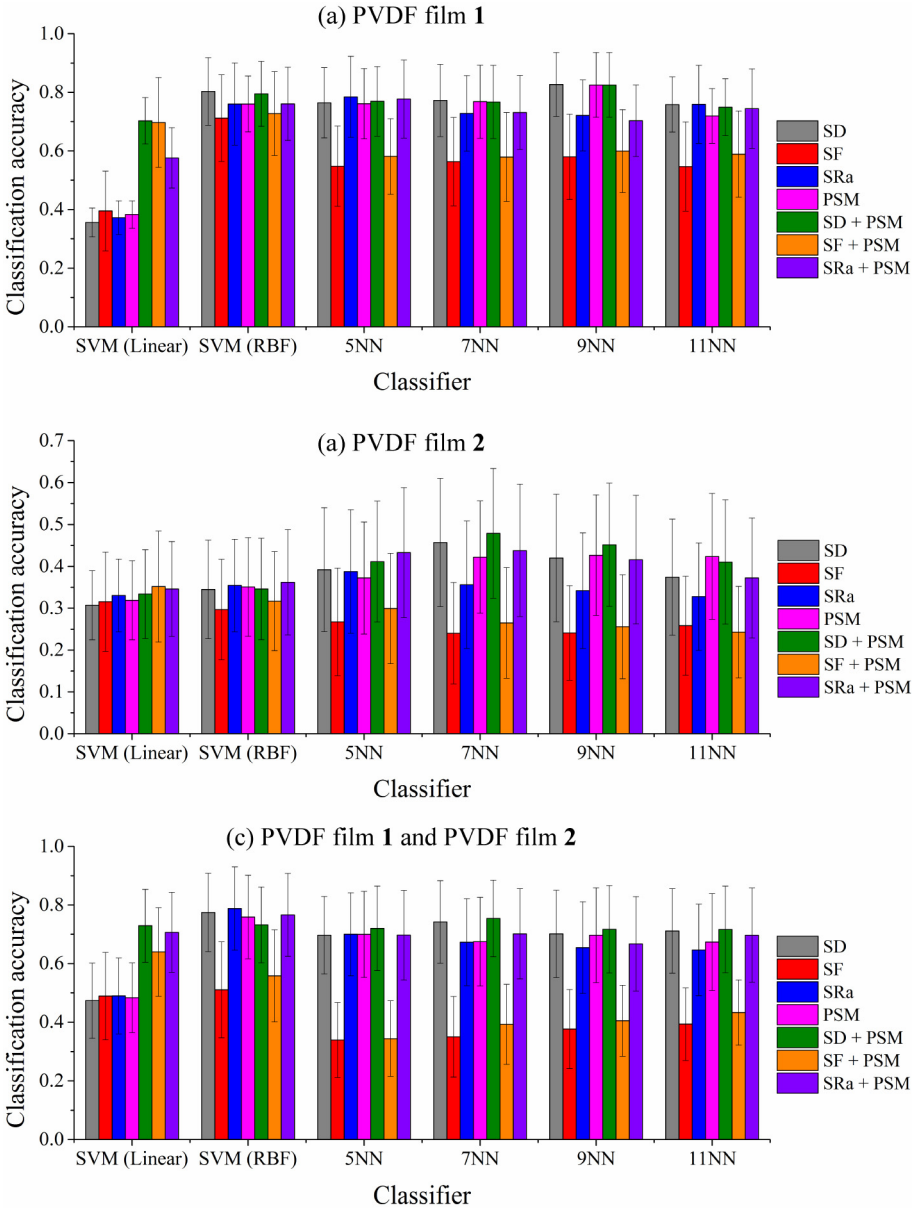

Fig. 7. Classification accuracy of each feature and classification algorithm with (a) only PVDF film 1, (b) only PVDF film 2, and (c) both PVDF film 1 and PVDF film 2. Error bars represent the standard error.

3.2.2. k-*Nearest neighbors (*k*NN)*

k-Nearest Neighbors is a non-parametric classifier. The class of a test sample is determined by taking majority vote of class labels among the *k* closest training samples. There are a variety of metrics to compute distance between samples such as Euclidean distance (L_2 distance), L_1 distance and cosine distance. In this paper, the Euclidean distance is employed. The choice of the value of *k* is crucial because a small *k* may lead to a classifier sensitive to noise samples, and a large *k* could result in less distinct boundaries between classes.

4. Experimental setup and protocol

The PVDF film sensor signals were amplified by a custom-built amplifier, and digitalized at a sampling rate of 1 kHz via an analog-to-digital converter (DAQCard USB-6225, National Instruments, USA). Supporting software was developed to record digital signals (LabVIEW, National Instruments, USA). Eight standard solid nickel test surfaces (Rubert & Co. Ltd., UK) with roughness values (Ra) of 50 μm (Surface 1), 25 μm (Surface 2), 12.5 μm (Surface 3), 6.3 μm (Surface 4), 3.2 μm (Surface 5), 1.6 μm (Surface 6), 0.8 μm (Surface 7), 0.4 μm (Surface 8) were explored (see Fig. 5). The test surface finish was carried out using cylindrical turning.

Experimental neuroscientists have identified lateral sliding movements play a vital role in mediating surface roughness recognition [12]. The cutaneous vibrations generated during the lateral sliding are encoded by the fast adapting mechanoreceptors. In this paper, we manually performed this simple sliding movement to explore the surface roughness (Fig. 1). This movement has been used for object identification as well [35,40]. During the experiments, the sliding direction, speed and contact pressure were roughly controlled by operator. The sliding speed in our experiments is around 0.24 m/s. We also observed that the magnitude of the signals will be smaller if the sliding speed is lower because the

Table 2
The highest classification accuracy based on both individual sensor and sensor combination.

Sensor	Feature	Classifier	Accuracy
PVDF film 1	SD	kNN (k = 9)	(82.6 ± 10.8)%
PVDF film 2	SD + PSM	kNN (k = 7)	(57.9 ± 15.2)%
PVDF film 1 + PVDF film 2	SRa	SVM (RBF)	(78.8 ± 14.2)%

frequency of vibration is smaller when the sliding speed is lower. The sliding speed and surface classification accuracy could be easily improved at the cost of including any speed controller. One PVDF film sensor was purposely put perpendicular to the sliding direction. The lateral sliding direction of the artificial fingertip along the test surface during our experiments is indicated by an arrow in Fig. 5. The Sample tactile signals generated by two PVDF films when laterally sliding on eight test surfaces with various roughness values are shown in Fig. 6. The PVDF film sensor parallel to the sliding direction is denoted by PVDF film 2, and the other PVDF film, which is close to the contact surface and perpendicular to PVDF film 2, is denoted by PVDF film 1.

5. Results and discussion

Ten lateral sliding movements were performed on the eight test surfaces, resulting in 80 tactile time series samples. For each test surface, the 10 tactile time series samples were randomly split into 9 samples as the training set and the remaining 1 sample as the test set. This split procedure was repeated 500 times. The feature vectors need to be normalized to avoid any bias among features and numerical difficulties during the calculation. The effects of extracted features, classification algorithms and sensor number were evaluated.

Fig. 7 shows the classification accuracy for each feature and algorithm with PVDF film 1 solely (Fig. 7(a)), PVDF film 2 solely (Fig. 7(b)), and both PVDF film 1 and PVDF film 2 (Fig. 7(c)). The highest classification accuracy using solely PVDF film 1 is (82.6 ± 10.8) % with kNN (k = 9) classifier and SD feature. In contrast, PVDF film 2 possesses a much weak discriminative capability, and the best classification accuracy is (57.9 ± 15.2) % with kNN (k = 7) classifier and SF + PSM feature. The highest recognition rate using the combination of PVDF film 1 and PVDF film 2 is (78.8 ± 14.2) % with SVM (RBF) classifier and SRa feature, i.e., the linear combination of two PVDF sensors on the feature level could not guarantee a performance improvement in terms of classification accuracy compared to the individual sensor. The accuracy of nonlinear feature combination such as multiple kernel learning [41,42] and boosting [32] could be evaluated in future work. In addition, the sensing direction of PVDF film 2 is perpendicular to the sliding direction, i.e., the short edge (28 μm) is perpendicular to the sliding direction, which could generate complex deformation in the much longer edge (4 mm) that strongly depends on the local conditions. As a result, the output signals generated from the deformation of film 2 are less reproducible, which lead to the reduced classification accuracy based on signals from film 2 as well as the combination with film 1. Table 2 summaries the highest classification accuracy based on both individual sensor and sensor combination. Table 3 and Table 4 respectively show the highest classification accuracy of each classifier and feature.

We take a closer look at the classification accuracy of each surface class in order to investigate the limitation of the developed approach. Fig. 8 shows the confusion matrix of the best classification results using the SVM classifiers (Fig. 8(a)) and the kNN classifiers (Fig. 8(b)). The majority of misclassifications are between surface 7 (Ra = 0.8 μm) and surface 8 (Ra = 0.4). In other words, our artificial fingertip is highly likely to classify surfaces with roughness above 1 μm. If these two surfaces are eliminated from the examined set, the best classification accuracy of the remaining six surface classes increases to 88.6% for the SVM (RBF) classifier with the SD feature and PVDF film 1 and 90.3% for the kNN (k = 9) classifier with the SD feature and PVDF film 1 respectively.

Table 3
The highest classification accuracy of each classifier.

Classifier	Feature	Sensor	Accuracy
SVM (Linear)	SD + PSM	PVDF film 1 + PVDF film 2	(72.9 ± 12.4)%
SVM (RBF)	SD	PVDF film 1	(80.3 ± 11.5)%
5NN	SRa	PVDF film 1	(78.5 ± 13.8)%
7NN	SD	PVDF film 1	(77.2 ± 12.3)%
9NN	SD	PVDF film 1	(82.6 ± 10.8)%
11NN	SRa	PVDF film 1	(75.9 ± 13.4)%

Table 4
The highest classification accuracy of each feature.

Feature	Classifier	Sensor	Accuracy
SD	kNN (k = 9)	PVDF film 1	(82.6 ± 10.8)%
SF	SVM (RBF)	PVDF film 1	(71.2 ± 14.7)%
SRa	SVM (RBF)	PVDF film1 + PVDF film 2	(78.8 ± 14.2)%
PSM	kNN (k = 9)	PVDF film 1	(82.5 ± 11.0)%
SD + PSM	kNN (k = 9)	PVDF film 1	(82.5 ± 11.0)%
SF + PSM	SVM (RBF)	PVDF film 1	(72.7 ± 14.3)%
SRa + PSM	kNN (k = 5)	PVDF film 1	(77.8 ± 13.3)%

6. Conclusion

We have presented an approach for performing tactile surface roughness discrimination with a biologically inspired artificial fingertip. The fabricated bioinspired fingertip has two PDMS layers with different stiffness. It contains a PMMA bar to mimic the bone and two perpendicular PVDF film sensors to be equivalent to fast adapting type I mechanorecepotors. The Ra value range of test surfaces is from 0.4 μm to 50 μm. Various types of features ranging from statistical features to spectral features are extracted from tactile signals, and two classification algorithms (SVM and kNN) are used. The best classification accuracy is (82.6 ± 10.8) % which can be obtained using only PVDF film 1 with kNN (k = 9) classifier and the SD feature. The classification accuracy could be enhanced to 90.3% using the kNN classifiers for surfaces with roughness larger than 1 μm. All the experimental data were collected by manually sliding the artificial fingertip on the testing surfaces without using any controller for either sliding speed or normal load, i.e., the developed approach is very affordable, robust and suitable for real time surface roughness evaluation, for example, during the polishing process of large propellers, which would not require the tedious work to move the samples to a roughness measurement platform.

Acknowledgments

This project is supported by the Joint PhD Degree Programme NTU–TU Darmstadt. The project is also supported by Fraunhofer Singapore, which is funded by the National Research Foundation (NRF) and managed through the multi-agency Interactive & Digital Media Programme Office (IDMPO) hosted by the Infocomm Media Development Authority of Singapore (IMDA). YL Zhang acknowledges the financial support of this research by the A*STAR AOP project (1223600005) and the A*STAR Industrial Robotics Programme (1225100007). Jan Peters acknowledges research funding from the European Community's Seventh Framework Programme (FP7) under grant agreements #610967 (TACMAN).

(a) Classifier: SVM (RBF) Feature: SD Sensor: PVDF film 1

	S1	S2	S3	S4	S5	S6	S7	S8	Accuracy
S1	492	8	0	0	0	0	0	0	98.4%
S2	0	467	33	0	0	0	0	0	93.4%
S3	0	0	452	48	0	0	0	0	90.6%
S4	0	0	41	343	116	0	0	0	68.6%
S5	0	0	0	88	412	0	0	0	82.4%
S6	0	0	0	0	6	494	0	0	98.8%
S7	0	0	0	0	0	0	388	112	77.6%
S8	0	0	0	0	0	11	325	164	32.8%

Overall Accuracy (Mean ± Standard deviation): (80.3 ± 11.5)%

(b) Classifier: *k*NN (*k* = 9) Feature: SD Sensor: PVDF film 1

	S1	S2	S3	S4	S5	S6	S7	S8	Accuracy
S1	500	0	0	0	0	0	0	0	100%
S2	0	500	0	0	0	0	0	0	100%
S3	0	81	419	0	0	0	0	0	83.3%
S4	0	0	45	373	82	0	0	0	74.6%
S5	0	0	0	88	412	0	0	0	82.4%
S6	0	0	0	0	0	500	0	0	100%
S7	0	0	0	0	0	0	429	71	85.8%
S8	0	0	0	0	0	0	326	174	34.8%

Overall Accuracy (Mean ± Standard deviation): (82.6 ± 10.8)%

S1 = Surface 1 (Ra = 50 μm)	S2 = Surface 2 (Ra = 25 μm)	S3 = Surface 3 (Ra = 12.5 μm)	S4 = Surface 4 (Ra = 6.3 μm)
S5 = Surface 5 (Ra = 3.2 μm)	S6 = Surface 6 (Ra = 1.6 μm)	S7 = Surface 7 (Ra = 0.8 μm)	S8 = Surface 8 (Ra = 0.4 μm)

Fig. 8. Confusion matrix of the best classification results of classification algorithms (a) the SVM classifier with RBF kernel, SD feature and PVDF film 1, and (b) the *k*NN classifier with $k = 9$, SD feature and PVDF film 1. The horizontal axis (S1-S8) denotes the ground truth, and the vertical axis represents the classifier output. The far right column presents the classification accuracy for each surface class.

References

[1] W. Tang, Y. Zhou, H. Zhu, H. Yang, The effect of surface texturing on reducing the friction and wear of steel under lubricated sliding contact, Appl. Surf. Sci. 273 (2013) 199–204.

[2] W.W. Mayol-Cuevas, J. Juarez-Guerero, S. Munoz-Gutierrez, A first approach to tactile texture recognition, IEEE Int. Conf. Syst. Man Cybern. 5 (1998) 4246–4250.

[3] H.B. Muhammad, C. Recchiuto, C.M. Oddo, L. Beccai, C.J. Anthony, M.J. Adams, M.C. Carrozza, M.C.L. Ward, A capacitive tactile sensor array for surface texture discrimination, Microelectron. Eng. 88 (2011) 1811–1813.

[4] F. De Boissieu, C. Godin, B. Guilhamat, D. David, C. Serviere, D. Baudois, Tactile texture recognition with a 3-axial force MEMS integrated artificial finger, Robot. Sci. Syst. (2009) 49–56.

[5] O. Kroemer, C.H. Lampert, J. Peters, Learning dynamic tactile sensing with robust vision-based training, IEEE Trans. Robot. 27 (2011) 545–557.

[6] C.M. Oddo, M. Controzzi, L. Beccai, C. Cipriani, M.C. Carrozza, Roughness encoding for discrimination of surfaces in artificial active-touch, IEEE Trans. Robot. 27 (2011) 522–533.

[7] E. Peiner, M. Balke, L. Doering, Slender tactile sensor for contour and roughness measurements within deep and narrow holes, IEEE Sens. J. 8 (2008) 1960–1967.

[8] T.V. Vorburger, H.-G. Rhee, T.B. Renegar, J.-F. Song, A. Zheng, Comparison of optical and stylus methods for measurement of surface texture, Int. J. Adv. Manuf. Technol. 33 (2007) 110–118.

[9] L. Skedung, M. Arvidsson, J.Y. Chung, C.M. Stafford, B. Berglund, M.W. Rutland, Feeling small: exploring the tactile perception limits, Sci. Rep. 3 (2013).

[10] C.E. Connor, K.O. Johnson, Neural coding of tactile texture: comparison of spatial and temporal mechanisms for roughness perception, J. Neurosci. 12 (1992) 3414–3426.

[11] T. Yoshioka, B. Gibb, A.K. Dorsch, S.S. Hsiao, K.O. Johnson, Neural coding mechanisms underlying perceived roughness of finely textured surfaces, J. Neurosci. 21 (2001) 6905–6916.

[12] X. Libouton, O. Barbier, Y. Berger, L. Plaghki, J.-L. Thonnard, Tactile roughness discrimination of the finger pad relies primarily on vibration sensitive afferents not necessarily located in the hand, Behav. Brain Res. 229 (2012) 273–279.

[13] G.J. Augustine, D.M. Chikaraishi, M.D. Ehlers, G. Einstein, D. Fitzpatrick, W.C. Hall, E. Jarvis, L.C. Katz, J. Kauer, A.-S. LaMantia, J.O. McNamara, R.D. Mooney, M.A.L. Nicolelis, D. Purves, P.H. Reinhart, S.A. Simon, J.H.P. Skene, J. Voyvodic, L.E. White, S.M. Williams, Neuroscience, 3rd ed., Sinauer Associates Inc, Massachusetts, 2004.

[14] K. Hosoda, Y. Tada, M. Asada, Anthropomorphic robotic soft fingertip with randomly distributed receptors, Rob. Auton. Syst. 54 (2006) 104–109.

[15] B. Jaffe, Piezoelectric Ceramics, 1st ed., Academic Press, New York, 1971.

[16] S. Sokhanvar, M. Packirisamy, J. Dargahi, A multifunctional PVDF-based tactile sensor for minimally invasive surgery, Smart Mater. Struct. 16 (2007) 989.

[17] K. Takashima, S. Horie, T. Mukai, K. Ishida, K. Matsushige, Piezoelectric properties of vinylidene fluoride oligomer for use in medical tactile sensor applications, Sens. Actuators A Phys. 144 (2008) 90–96.

[18] A. Bonakdar, N. Narayanan, Determination of tissue properties using microfabricated piezoelectric tactile sensor during minimally invasive surgery, Sens. Rev. 30 (2010) 233–241.

[19] C. Li, P.-M. Wu, S. Lee, A. Gorton, M.J. Schulz, C.H. Ahn, Flexible dome and bump shape piezoelectric tactile sensors using PVDF-TrFE copolymer, J. Microelectromech. Syst. 17 (2008) 334–341.

[20] R.D. Howe, M.R. Cutkosky, Dynamic tactile sensing: perception of fine surface features with stress rate sensing, IEEE Trans. Robot. Autom. 9 (1993) 140–151.
[21] B. Choi, H.R. Choi, S. Kang, Development of tactile sensor for detecting contact force and slip, IEEE/RSJ Int Conf. Intell. Robot. Syst. 263 (2005) 2638–2643.
[22] A. Kimoto, N. Sugitani, S. Fujisaki, A multifunctional tactile sensor based on PVDF films for identification of materials, IEEE Sens. J. 10 (2010) 1508–1513.
[23] Z. Yi, Y. Zhang, Bio-inspired tactile FA-I spiking genertion under sinusoidal stimuli, J. Bionic Eng. 13 (2016) 612–621.
[24] S. Najarian, J. Dargahi, A.A. Mehrizi, Artificial Tactile Sensing in Biomedical Engineering, 1st ed., McGraw-Hill Education, New York, 2009.
[25] Q. Xu, C. Li, Y. Kang, Y. Zhang, Long term effects of substrate stiffness on the development of hMSC mechanical properties, RSC Adv. 5 (2015) 105651–105660.
[26] S.B. Davis, P. Mermelstein, Comparison of parametric representations for monosyllabic word recognition in continuously spoken sentences, IEEE Trans. Acoust. Speech Signal Process. 28 (1980) 357–366.
[27] D.G. Lowe, Distinctive image features from scale-invariant keypoints, Int. J. Comput. Vis. 60 (2004) 91–110.
[28] P. Dallaire, P. Giguère, D. Émond, B. Chaib-Draa, Autonomous tactile perception: a combined improved sensing and Bayesian nonparametric approach, Rob. Auton. Syst. 62 (2014) 422–435.
[29] S. Salehi, J.-J. Cabibihan, S.S. Ge, Artificial skin ridges enhance local tactile shape discrimination, Sens. (Basel). 11 (2011) 8626–8642.
[30] K. Englehart, B. Hudgins, P.A. Parker, M. Stevenson, Classification of the myoelectric signal using time-frequency based representations, Med. Eng. Phys. 21 (1999) 431–438.
[31] K. Schaaff, T. Schultz, Towards an EEG-based emotion recognizer for humanoid robots, in: 18th IEEE Int. Symp. Robot Hum. Interact. Commun., 2009, pp. 792–796.
[32] P. Gehler, S. Nowozin, On feature combination for multiclass object classification, in: IEEE 12th Int. Conf. Comput. Vis., 2009, pp. 221–228.
[33] J. Ngiam, A. Khosla, M. Kim, J. Nam, H. Lee, A.Y. Ng, Multimodal deep learning, in: Proc 28th Int. Conf. Mach. Learn., 2011, pp. 689–696.
[34] A. Drimus, M.B. Petersen, A. Bilberg, Object texture recognition by dynamic tactile sensing using active exploration, in: 21st IEEE Int. Symp. Robot Hum. Interact. Commun., 2012, pp. 277–283.
[35] J. Hoelscher, J. Peters, T. Hermans, Evaluation of tactile feature extraction for interactive object recognition, in: IEEE-RAS 15th Int. Conf. Humanoid Robot., 2015, pp. 310–317.
[36] F. Veiga, H. van Hoof, J. Peters, T. Hermans, Stabilizing novel objects by learning to predict tactile slip, in: IEEE/RSJ Int. Conf. Intell. Robot. Syst., 2015, pp. 5065–5072.
[37] C. Cortes, V. Vapnik, Support vector machine, Mach. Learn. 20 (1995) 273–297.
[38] C.-W. Hsu, C.-J. Lin, A comparison of methods for multiclass support vector machines, Neural Netw. IEEE Trans. 13 (2002) 415–425.
[39] C.-C. Chang, C.-J. Lin, LIBSVM: a library for support vector machines, ACM Trans. Intell. Syst. Technol. 2 (2011) 27.
[40] J. Edwards, J. Lawry, J. Rossiter, C. Melhuish, Extracting textural features from tactile sensors, Bioinspir. Biomim. 3 (2008) 35002.
[41] A. Rakotomamonjy, F. Bach, S. Canu, Y. Grandvalet, M.K.L. Simple, J. Mach. Learn. Res. 9 (2008) 2491–2521.
[42] M. Gönen, E. Alpaydın, Localized algorithms for multiple kernel learning, Pattern Recognit. 46 (2013) 795–807.

Biographies

Zhengkun Yi received his B.S. degree (2009) from University of Science and Technology of China (USTC) and M.E. degree (2012) from Chinese Academy of Sciences (CAS). He is currently a PhD student in the joint PhD degree programme between Nanyang Technological University (NTU) and Technische Universitaet Darmstadt (TUDa). His research interests include biomimetic tactile sensing and exploration, sensor fabrication technologies, machine learning, and computational neuroscience.

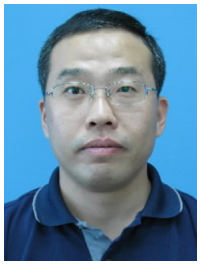

Yilei Zhang received his Ph.D degree (2007) from Iowa State University in mechanical engineering and electrical engineering. Before joining Nanyang Technological University in 2012, he served as a senior research engineer in the Goodyear Tire and Rubber Company. His research interests include neuroengineering, bioinspired sensors, etc.

Jan Peters is a Full Professor (W3) for Intelligent Autonomous Systems at the Computer Science Department of the Technische Universitaet Darmstadt and at the same time a senior research scientist and group leader at the Max-Planck Institute for Intelligent Systems, where he heads the interdepartmental Robot Learning Group. Jan Peters has received the Dick Volz Best 2007 US Ph.D. Thesis Runner-Up Award, the 2012 Robotics: Science & Systems – Early Career Spotlight, the 2013 INNS Young Investigator Award, and the IEEE Robotics & Automation Society's 2013 Early Career Award. In 2015, he was awarded an ERC Starting Grant. Jan Peters has studied Computer Science, Electrical, Mechanical and Control Engineering at TU Munich and FernUni Hagen in Germany, at the National University of Singapore (NUS) and the University of Southern California (USC), and been an visiting researcher at the ATR Telecommunications Research Center in Japan. He has received four Master's degrees in these disciplines as well as a Computer Science PhD from USC.